PAPER • **OPEN ACCESS**

Accessible power for medical equipment in remote healthcare: a solution for single-phase power generation using three-phase induction machines

To cite this article: Bruno Romeiro *et al* 2026 *Eng. Res. Express* **8** 055302

Engineering Research Express

OPEN ACCESS

RECEIVED
22 September 2025

REVISED
8 February 2026

ACCEPTED FOR PUBLICATION
18 February 2026

PUBLISHED
3 March 2026

PAPER

Accessible power for medical equipment in remote healthcare: a solution for single-phase power generation using three-phase induction machines

Bruno Romeiro[1,2,*], **Carlos Oliveira**[2,3], **Cicero Hildenberg**[2,3], **Ângela Ferreira**[1,3] and **Francisco Filho**[2,3]

[1] CeDRI, SusTEC, Instituto Politécnico de Bragança, 5300-253 Bragança, Portugal
[2] LINMET, Universidade Tecnológica Federal do Paraná, 86812-460, Apucarana, Paraná, Brasil
[3] These authors contributed equally to this work.
[*] Author to whom any correspondence should be addressed.

E-mail: brunoeduardo775@gmail.com, carlosoliveira@utfpr.edu.br, hildenberg@utfpr.edu.br, apf@ipb.pt and franciscofilho@alunos.utfpr.edu.br

Keywords: medical care, remote areas, low cost generator, induction machine

Abstract

This work was motivated by the urgent need for reliable electricity in remote areas where conventional power distribution, and consequently access to healthcare, remains impractical. The proposed system is a practical alternative to conventional synchronous generators commonly used in off-grid applications, which have high implementation and maintenance costs and potential risks in healthcare applications due to the spark generated by the brushes. We propose the use of a self-excited single-phase generator, derived from a three-phase induction machine, as a robust, low-cost, highly reliable and safe solution for supplying electrical power to medical applications in remote locations. The work presents a mathematical model based on the theory of symmetrical components, which incorporates frequency variation and unbalanced system operation, along with an analytical methodology to determine the capacitance values required for this application and all system elements, including the definition of the sizing factors K_E and K_M. The proposed approach allows for rigorous design without relying on empirical procedures as commonly presented in the literature, and is experimentally validated using real medical loads. Our experimental setup incorporates current medical devices, including three infusion pumps, a cardioverter-defibrillator, and a patient monitoring device. Despite modest voltage imbalances observed during steady-state operation, all medical devices maintained adequate functionality during testing. The transient response during load switching showed damped oscillations before returning to steady-state operation, demonstrating stable voltage and frequency behavior without the use of active electronic control. The generator demonstrated satisfactory voltage regulation and short-circuit self-protection capabilities without the need for complex systems, making it economically viable for deployment in resource-constrained environments. These results suggest that the proposed configuration offers a practical solution for the electrification of medical facilities in regions where grid extension remains challenging or prohibitively expensive.

1. Introduction

The need for low-cost power generation systems in remote locations represents a significant challenge, especially in developing countries [1], directly impacting the health and well-being of millions of people. In Brazil, for example, many isolated communities are located in rural areas along lakes and rivers, often more than 500 km away from urban centers. These riverside populations often lack regular access to essential public services, including health, education, and sanitation. Consequently, to receive medical care - centralized in

municipal centers - residents must embark on long journeys that can last days or weeks, aggravating health risks in emergency situations [2–4].

In these circumstances, autonomous power generation systems become essential to enable the operation of critical medical equipment, vital for the timely diagnosis and treatment of common diseases, as well as for safe childbirth and neonatal care [5]. Among the potential solutions for off-grid power generation, where the costs of extending transmission infrastructure is prohibitively high, synchronous machines coupled with combustion engines are often used [6, 7].

In healthcare applications, where financial resources are limited, systems based on synchronous machines may become unfeasible due to the need for components for voltage regulation control and system grounding, high acquisition costs, and maintenance requirements due to the use of brushes and field windings [8–10]. Beyond the high cost, these characteristics contribute to low supply reliability, as operational failures can lead to power interruptions, potentially with fatal consequences in the healthcare area.

Among the potential research areas, we have the squirrel-cage three-phase induction machine (TIM), which is of interest to scientific and industrial communities for applications in actuators or power generation systems [6]. TIMs operating as a self-excited induction generator (SEIG) offers significant advantages in terms of reliability, with a squirrel-cage rotor that eliminates brushes, slip rings, and field windings, in addition to operational advantages due to its robustness, simplicity of construction, low maintenance, high power density, and low cost [11–13]. The use of TIMs remains viable and technically advantageous, also when compared to single-phase induction machines, due to their higher energy efficiency [14, 15], increasing the autonomy of the system. However, SEIGs suffer from unsatisfactory voltage regulation and frequency variations and are therefore only suitable for constant speed and load applications [16, 17]. The robust design [18, 19], combined with lower manufacturing costs, simplified operation, high efficiency, and inherent protection against overload and short circuit [15, 20, 21], makes SEIGs the most suitable option for medical applications when all the system components are sized correctly.

In general, medical equipment requires single-phase power supplies. In the literature, we find the use of SEIGs to power single-phase loads, and three of the main connections are proposed by Steinmetz [22, 23], Smith [24, 25] and Fukami [10, 23, 26]. Other works present studies that demonstrate configuration variations showing good applicability for this form of SEIG use in single-phase configuration [27–31]. The Fukami connection has been widely investigated and applied in power generation systems, due to its ability to improve electrical performance through the use of capacitor banks [32, 33]. Some current and relevant works in the literature use this topology as the main basis for study [6, 34, 35] adopting capacitor values or capacitance ratios as proposed by Fukami in 1995. However, this type of connection has never been applied to medical equipment that requires certain restrictions on power supply. Furthermore, the literature only addresses empirical methods for defining excitation capacitors, which can be detrimental for loads that require specific power quality levels. In this context, the study and evaluation of the use of self-excited induction generators in electrical systems gain relevance as a viable alternative that contributes to energy resilience, especially when seeking low cost, simplicity, reliability, and safety.

This work proposes the use of a TIM operating as a SEIG, based on the three-phase Fukami connection [10, 23], as a means to supply of single-phase power. Unlike previous works [6, 21, 36], this article proposes a methodology for defining the components of a low-cost generation system, in order to ensure the continuous and reliable operation of medical equipment, while meeting the power quality standards specified by equipment manufacturers. The main contributions offered by this work can be summarized as follows:

- Proposal for an off-grid power generation system based on a SEIG operating as a single-phase generator to provide healthcare in remote areas. Solution that exploits the robustness and passive self-protection characteristics of the self-contained generator, increasing operational reliability in clinical environments, reducing maintenance requirements and the Levelized Cost of Energy (LCOE), compared to solutions commonly employed in remote regions.
- The proposed system ensures stable voltage and frequency behavior without the use of active electronic control.
- Development of a predictive mathematical model based on the Theory of Symmetrical Components, allowing for the systematic analysis of unbalanced generator operation and reducing the reliance on empirical procedures during the design and deployment of the system in the field.
- Practical methodology for sizing all system elements, including excitation capacitors, main TIM rated power, prime mover, and the definition of the sizing factors K_E and K_M. Enabling the reproduction of the system for different power levels.

Table 1. Medical equipment and its typical power ratings in intensive care units.

Equipment name	Active power (W)	Reactive power (vAr)
Multiparameter Monitor[1]	50–80	10–20
Defibrillator[2]	70–150	20–40
Infusion Pump [3]	20–30	5–10
Syringe Pump[4]	4–5	1–3
Feeding Pump[5]	1.5–2	< 1
Ventilator (basic)[6]	74	15–25
Ventilator (with humidifier)[7]	149	30–50
Portable US Scanner[8]	300–800	80–200
CRRT / Dialysis Machine[9]	1300–1500	300–400
Pulse-Oximeter[10]	3–8	1–3
ECG Machine (12-lead)[11]	25–40	5–10
CPAP / BiPAP Unit[12]	60–150	15–40

- Experimental validation of the proposed methodology using critical medical equipment, including infusion pumps, a cardioverter-defibrillator, and a multiparameter patient monitor.

2. Clinical requirements for ICU power supply systems

Intensive Care Units (ICUs) rely on numerous electrically powered devices, including life-support systems, ventilators, infusion pumps (syringe and peristaltic), cardioverter-defibrillators, multiparameter monitors, point-of-care ultrasound units, and continuous renal replacement therapy equipment, whose collective power consumption is relatively small compared to their clinical importance (table 1). Even brief power interruptions lasting only seconds can lead to severe hypoxemia, cardiovascular instability, or critical loss of physiological monitoring data [37]. Accordingly, international guidelines for healthcare facility electrification categorize these devices as critical loads, mandating their continuous power availability through uninterruptible pathways. Design standards thus require automatic transfer switches and energy storage systems capable of maintaining an uninterrupted power supply for at least 48 h in tertiary-level hospitals [38].

The proposed system configuration reduces the chance of failures. First, the stator and rotor cage currents must remain below the thermal limit under sustained fault conditions, avoiding insulation degradation, accelerated temperature rise in conductors, and thermal deformation of the rotor, all of which significantly reduce generator service life; second, no arcing or hot spots can be created that could ignite fuel vapors or combustible polymers inside the equipment enclosures. Furthermore, the capacitive self-excitation bank must be dimensioned so that a three-phase fault to ground forces the terminal voltage to collapse safely, avoiding ferroresonance or overvoltage transients during fault clearance. The proposed robust generation system significantly reduces the risk of failures and has the terminal voltage collapsed during a short circuit, ensuring greater reliability and safety in healthcare applications.

In addition to fault tolerance, power quality has a decisive influence on measurement accuracy and actuator reliability. The infusion pumps listed in table 1, for example, use stepper motors driven by switched-mode power supplies that tolerate 90-264 Vrms, [39, 40]. Ventilators are even more sensitive: fan speed regulation relies on the detection of reverse sinusoidal electromotive force and can desaturate if the total harmonic distortion (THD) exceeds 8-10%, distorting its waveform and introducing non-sinusoidal components that are not correctly interpreted by the control circuit. Consequently, zero-crossing detection algorithms, speed estimation routines, or Back-EMF filtering processes operate outside their design conditions. Consequently, the proposed TIM-based generator must provide an output voltage V_{out} determined by the equipment requirements with low voltage variation, being $\pm 5\%$ and THD $< 5\%$ [38]

Finally, fire safety is intrinsically linked to generator efficiency: lower copper losses translate into cooler surfaces, reducing the likelihood of ignition in oxygen-enriched atmospheres often present near ventilated patients [41]. Empirical data from rural Brazilian health centers show that a 3 kW SEIG operating at 83% efficiency maintains surface temperatures approximately 50 °C below the autoignition limit of common polymeric enclosures [42]. The brushless design of the TIM avoids the operational sparks associated with conventional synchronous generators, resulting from mechanical contact between brushes and slip rings. Therefore, by combining prudent thermal design with coordinated protection devices, the proposed power

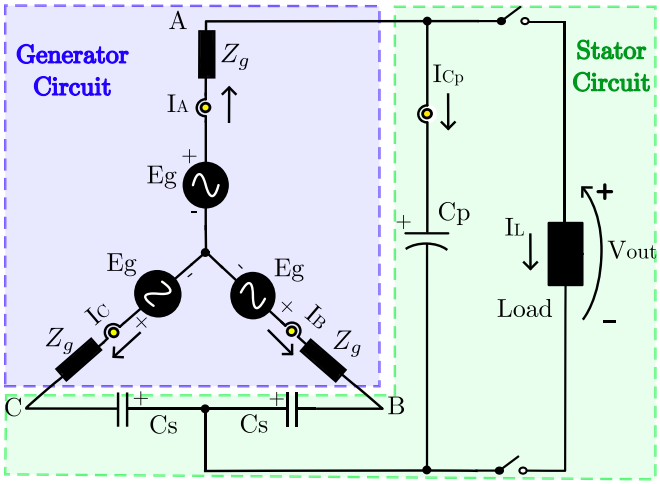

Figure 1. Fukami conection for SEIG.

generation architecture meets the requirements of uninterrupted operation and intrinsic fireproof behavior, both essential for the protection of patients in resource-limited ICUs.

Corresponding brands/models for superscripts in the table 1: [1] Alfamed *VITA*; [2] *CardioStart*; [3] *Medicatec*; [4] Fresenius *Agilia*; [5] Fresenius *Amika*; [6] Hamilton *C6*; [7] Hamilton *C6+H-900*; [8] GE/Philips (típ.); [9] *Diapact/Prismaflex*; [10] Hand-held; [11] GE/Nihon Koden; [12] ResMed/Philips;

3. Mathematical modeling of three-phase induction generator with single-phase connection

Considering that the health area has specific and demanding operational conditions regarding voltage stability and power conditions, this section presents the development of the mathematical model of the TIM operating as a single-phase generator as shown in figure 1.

3.1. Stator circuit

The symmetrical components method, based on Fortescue's Theorem, was chosen to model the system, as it operates in an unbalanced manner due to the supply of single-phase loads by a three-phase generator. As shown in figure 1, the generator is connected in a star configuration, and because it is an isolated and self-excited generator, the symmetrical components matrices for voltage and current are independent of the zero sequence component, since there is no connection between the generator's neutral and the load. Thus, the equations for the phase currents are defined in terms of the positive and negative sequence currents, I_{1p} and I_{1n} respectively, being $\alpha = e^{j2\pi/3}$ the phase shift between phases. Therefore, the stator currents in symmetrical components are as follows:

$$\begin{cases} I_A = 1 \cdot I_{1p} + 1 \cdot I_{1n} \\ I_B = \alpha^2 \cdot I_{1p} + \alpha \cdot I_{1n} \\ I_C = \alpha \cdot I_{1p} + \alpha^2 \cdot I_{1n} \end{cases} \tag{1}$$

The line voltages at the generator output, V_{AB}, V_{BC}, and V_{CA}, can also be expressed in terms of symmetrical components, using the phase currents defined by (1), as follows:

$$\begin{cases} V_{AB} = Z_e \cdot I_A + j \cdot x_{cs} \cdot I_B \\ V_{BC} = -j \cdot x_{cs} \cdot I_B + j \cdot x_{cs} \cdot I_C \\ V_{CA} = -j \cdot x_{cs} \cdot I_C - Z_e \cdot I_A \end{cases} \tag{2}$$

Z_e corresponds to the equivalent impedance of the parallel arrangement of capacitor *Cp* with the load, and x_{cs} represent the reactance of capacitor *Cs*, given by $x_{cs} = -\frac{1}{2\pi f_r C_s}$, where f_r is the rated frequency of generation.

Therefore, the stator voltages in positive sequence (V_{1p}) and negative sequence (V_{1n}) symmetrical components are given by the following matrix:

$$V_{1p_{\text{stator}}} = (1 - \alpha^2) \cdot \left[\frac{I_{1p}}{3}(Z_e - 2jx_{cs}) + \frac{I_{1n}}{3}(Z_e + jx_{cs}) \right] \tag{3}$$

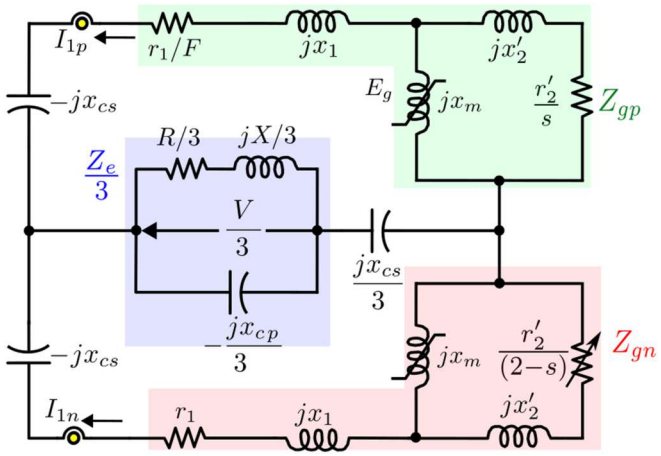

Figure 2. Machine equivalent circuit.

$$V_{1n_{\text{stator}}} = (1-\alpha)\cdot\left[\frac{I_{1p}}{3}(Z_e + jx_{cs}) + \frac{I_{1n}}{3}(Z_e - 2jx_{cs})\right] \tag{4}$$

3.2. Generator circuit

It is also possible to formulate the voltages generated in positive and negative sequence by using the equivalent internal impedance Z_g for each phase, which depends directly on the machine's characteristics, observed in figure 2. With E_g being the air gap voltage, from figure 1, we express the line voltages as a function of the impedance Z_g and phase currents from (1).

$$\begin{cases} V_{AB} = -Z_g \cdot I_{1p} \cdot (\alpha^2 - \alpha) - Z_g \cdot I_{1n} \cdot (\alpha - \alpha^2) \\ V_{BC} = -Z_g \cdot I_{1p} \cdot (\alpha - 1) - Z_g \cdot I_{1n} \cdot (\alpha^2 - 1) \\ V_{CA} = -Z_g \cdot I_{1p} \cdot (1 - \alpha^2) - Z_g \cdot I_{1n} \cdot (1 - \alpha) \end{cases} \tag{5}$$

It is possible to express the internal generator voltages in their sequence components in the same way as the line voltages, as follows:

$$V_{1p_{\text{gen}}} = \frac{1}{3}(V_{CA} + \alpha V_{AB} + \alpha^2 V_{BC}) = -(1-\alpha^2)Z_{gp}I_{1p} \tag{6}$$

$$V_{1n_{\text{gen}}} = \frac{1}{3}(V_{CA} + \alpha^2 V_{AB} + \alpha V_{BC}) = -(1-\alpha)Z_{gn}I_{1n} \tag{7}$$

Where Z_{gp} and Z_{gn} are thepositive and negative sequence internal impedances, respectively.

3.3. Equivalent circuit

To obtain the equivalent circuit representation of the single-phase machine, we equate the positive sequences (3) and (6) and negative sequences (4) and (7) of the generator and stator.

$$\begin{aligned} V_{1p_{\text{stator}}} = V_{1p_{\text{gen}}} I_{1p} \cdot \left(\frac{Z_e}{3} - \frac{2}{3}j \cdot x_{cs} + Z_{gp}\right) \\ + I_{1n} \cdot \left(\frac{Z_e}{3} + j \cdot \frac{x_{cs}}{3}\right) = 0 \end{aligned} \tag{8}$$

$$\begin{aligned} V_{1n_{\text{stator}}} = V_{1n_{\text{gen}}} I_{1p} \cdot \left(\frac{Z_e}{3} + j \cdot \frac{x_{cs}}{3}\right) \\ + I_{1n} \cdot \left(\frac{Z_e}{3} - \frac{2}{3}j \cdot x_{cs} + Z_{gn}\right) = 0 \end{aligned} \tag{9}$$

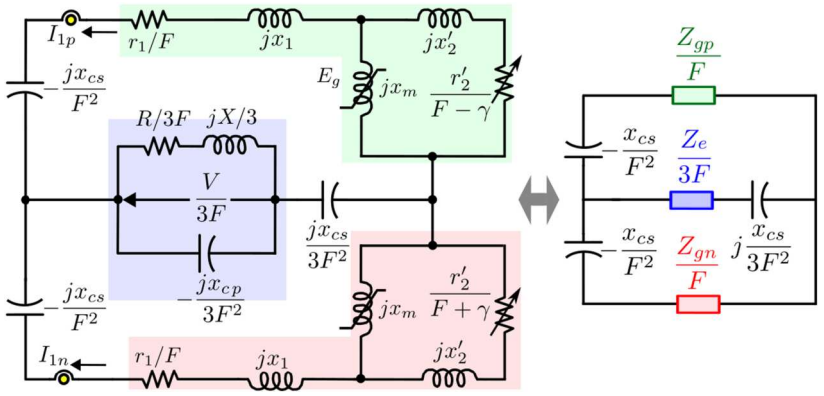

Figure 3. Equivalent circuit with frequency variation.

Consequently, the matrix using the (8) and (9) is as follows:

$$\begin{bmatrix}0\\0\end{bmatrix}=\begin{bmatrix}a & b\\ c & d\end{bmatrix}\cdot\begin{bmatrix}I_{1p}\\ I_{1n}\end{bmatrix}\Rightarrow\begin{cases}a=\frac{Z_e}{3}-\frac{2}{3}j\cdot x_{cs}+Z_{gp}\\ b=\frac{Z_e}{3}+j\cdot\frac{x_{cs}}{3}\\ c=\frac{Z_e}{3}+j\cdot\frac{x_{cs}}{3}\\ d=\frac{Z_e}{3}-\frac{2}{3}j\cdot x_{cs}+Z_{gn}\end{cases}\tag{10}$$

The impedances Z_{gp} and Z_{gn}, are part of the equivalent circuit, varying according to the slip s and the magnetization reactance x_m. In this way, the equivalent circuit is obtained by analyzing the path taken by the currents I_{1p} and I_{1n} for operation at rated frequency f_r, observed in figure 2, which facilitates the analysis of the machine circuit.

However, to include the effect of frequency variation according to load variation, the term $F=\frac{f}{f_r}$ which represents the frequency variation per unit, where f is the frequency of the generated voltage, and the term $\gamma=\frac{\omega}{\omega_r}$ which represents the rotor speed per unit, with ω being the rotor angular speed and $\omega_r=2\pi f_r$ the rated angular speed, are included in the equivalent circuit. With $\omega_s=2\pi f$ being the generating angular speed, the slip s is defined as $s=\frac{\omega_s-\omega}{\omega_s}=\frac{F-\gamma}{F}$. Thus, the final result of the generator equivalent circuit is obtained as shown in figure 3. Based on this equivalent circuit, the steady-state characteristics of the generator are calculated.

To determine the parameters of the magnetization branch of the equivalent circuit, E_g and x_m, and also the frequency variation F for each load, capacitance and rotor speed, we can analyze the total impedance Z of the circuit as seen by the current I_{1p} [43, 44]. In off-grid systems, the terminal voltage is sustained by self-excitation via capacitors, and the current I_{1p} flows even without an external voltage source. Applying Kirchhoff's Law, we have $Z\cdot I_{1p}\approx 0$ since only the voltage E_g operates as a system source, which implies $Z\approx 0$ for $I_{1p}\neq 0$, where Z is given by:

$$Z=\frac{Z_{gp}}{F}-\frac{jx_{cs}}{F^2}+\frac{\left(\frac{Z_{gn}}{F}-\frac{jx_{cs}}{F^2}\right)\cdot\left(\frac{Z_e}{F}+\frac{jx_{cs}}{3F^2}\right)}{\frac{Z_{gn}}{F}-\frac{jx_{cs}}{F^2}+\frac{Z_e}{F}+\frac{jx_{cs}}{3F^2}}\tag{11}$$

By using the previous equation, it is possible to obtain two nonlinear equations with x_m and F as variables for each value of load, capacitance and rotor speed. Solving this equation with the lqsnonlin function in MATLAB, seeking to zero the real and imaginary parts of Z, we find x_m and F that characterize the behavior of the machine for each specific operating point [43–45].

With x_m and F determined for power generation, we can identify the air-gap voltage E_g for each x_m. The curve E_g x x_m, and also all the TIM parameters used in this work, obtained through tests presented in [18, 46], are presented in Appendix. With E_g obtained in figure A.1, and the other variable parameters determined for each specific operating point, it is possible to analyze the generator characteristics using the following equations:

$$I_{1p}=\frac{E_g}{\frac{r_1}{F}+jx_1-\frac{jx_{cs}}{F^2}+\frac{\left(\frac{Z_{gn}}{F}-\frac{jx_{cs}}{F^2}\right)\cdot\left(\frac{Z_e}{F}+\frac{jx_{cs}}{3F^2}\right)}{\left(\frac{Z_{gn}}{F}-\frac{j2x_{cs}}{3F^2}+\frac{Z_e}{F}\right)}}\tag{12}$$

$$I_{1n} = -\frac{\frac{Z_e}{3F} + \frac{jx_{cs}}{3F^2}}{\frac{Z_{gn}}{F} + \frac{Z_e}{3F} - \frac{j2x_{cs}}{3F^2}} \cdot I_{1p} \tag{13}$$

The load current is given by:

$$I = -\frac{\frac{jx_{cs}}{F^2}}{\frac{R}{F} + jX - j\frac{x_{cp}}{F^2}} \cdot (I_{1p} + I_{1n}) \tag{14}$$

Finaly, the generator voltage and output power can be expressed as:

$$V_{out} = (R + j \cdot X \cdot F) \cdot I \tag{15}$$

$$P_{out} = |I|^2 \cdot R \tag{16}$$

Equations (15) and (16) are fundamental for the analysis and validation of the proposed generation system. They enable the prediction of voltage bahaviour at the load connection point, while accounting for the inherent imbalance of the configuration. This approach makes it possible to assess whether the system meets the necessary criteria for the safe and effective operation of medical equipment under various operating conditions.

4. Induction generator features for medical applications

4.1. Self-excitation phenomenon

The connection of a capacitor bank with significant capacitance to the stator terminals, together with the presence of remanent magnetic flux density in the rotor iron and the driving of the prime mover, triggers the induction of an electromotive force (EMF) in the stator windings of the machine [47, 48]. If the magnitude of this EMF is sufficiently high, primary electric currents will flow through the capacitor bank.

The magnetic flux resulting from these currents will act to sustain and reinforce the residual magnetism present in the rotor. Consequently, the currents induced in the machine will increase progressively, a process that feeds back positively, until the generator reaches a steady-state voltage [49].

In SEIGs, the terminal voltage is sustained by the magnetizing current, supplied by the capacitor bank. When a load is connected to the generator, part of the available current is used to power the load, reducing the magnetizing current and, consequently, the voltage maintenance capacity. However, medical devices become favorable for applications involving SEIG because they have low collective energy consumption - as presented in section 2 - which is reflected in low currents demanded by these loads. This promotes a low reduction in the magnetizing current circulating through the capacitor bank, allowing the magnetic flux level in the air gap to be maintained within an adequate range. As a result, after the load connection, the terminal voltage experiences a minimal drop, stabilizing in steady state.

Thanks to the phenomenon of self-excitation, the generator set becomes significantly more economical and simplified, since it eliminates the need for voltage excitation sources and allows the use of squirrel-cage rotors. The absence of complex electronic components and auxiliary circuits also contributes to cost reduction and higher reliability of the system, making it a viable and attractive alternative for off-grid applications in the health area.

4.2. Voltage regulation analysis

Based on the mathematical modeling presented in section 3, and the TIM parameters, presented in table A1 of Appendix, is possible to determine the variation of the terminal voltage as a function of the power supplied to the load, observed in figure 4. For each new value assigned to the load and capacitances' specification, the system of equations is solved, resulting in the corresponding output voltage. In this way, the curve V_{out} versus P_{out} is obtained, which faithfully represents the system response to the demand of different power values.

These curves provide essential information for evaluating voltage regulation in steady state, especially in isolated systems with sensitive loads, such as those used for medical applications. By observing the slope and limits for medical applications, it is possible to identify the safe operating ranges, in which the voltage remains within the admissible values for the connected equipment. Furthermore, the analysis for different capacitance configurations (values of C_p and C_s) allows us to observe that for a ratio of 62.6%—obtained by $\frac{|C_p - C_s|}{C_p}$—between C_s and C_p as proposed in [26], better voltage regulation is obtained, which directly affects the system's ability to sustain the voltage under load.

Although the proposed topology inherently possesses a three-phase voltage imbalance in the TIM, this condition does not affect the connected load. Medical devices are powered by a regulated single-phase voltage, derived directly from the generator output, which must maintain stable amplitude and frequency within the limits specified by the manufacturers. Therefore, medical equipment is not exposed to three-phase voltage

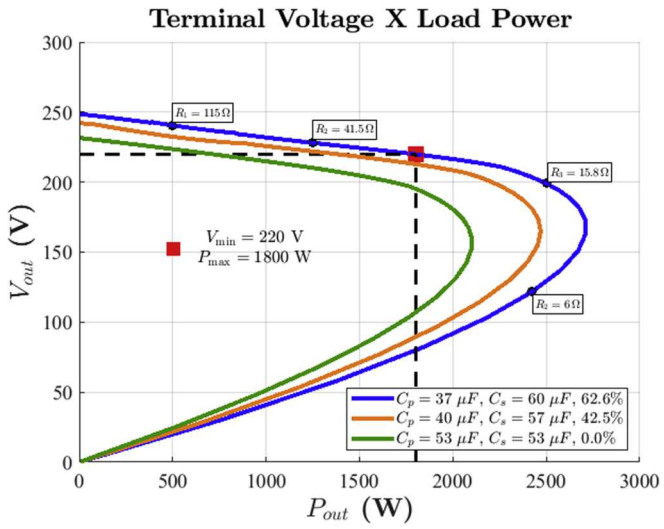

Figure 4. Output voltage variation V_{out} with increasing load power P_{out}.

imbalance, which prevents thermal stress or aging of the components. The effects of voltage imbalances only affect the generator itself, manifesting as small current asymmetries between the stator windings, which must remain within the machine's nominal operating limits.

By analyzing the points $V_{\min}$ and $P_{\max}$, obtained for the best relationship between C_p and C_s, it is possible to design a system that operates at the appropriate point of the desired output voltage V_{out}, avoiding undersizing and ensuring stability and safety throughout the operation.

This approach is advantageous because it allows the application of a low-cost system, enabling its use in scenarios that require flexibility, such as mobile intensive care units (ICUs), where the energy demand can vary depending on the connected medical equipment. The possibility of resizing the system in a practical and safe way, as needed, reinforces the potential application of this methodology in mobile and adaptable power generation systems.

4.3. Short-circuit behavior

In many conventional systems, a set of specific components and infrastructure are required. To avoid damage to the synchronous generator and connected systems, fast circuit breakers, dedicated protection systems, and additional control schemes are often necessary, increasing the cost, complexity, and maintenance requirements of the installation. Therefore, unlike conventional synchronous generators that provide continuous voltage generation even under short circuits, in the proposed system, the dynamics of the TIM itself mitigate the effects of a severe fault, eliminating such requirements and contributing to increased accessibility, reduced total costs and fire risk.

Different of conventional synchronous generators, the generation set proposed in this work has an intrinsic characteristic of self-protection against short circuits [20, 21, 43, 50]. This process occurs naturally, without the need for additional sensors, complex measurement systems, or dedicated microprocessors for protection detection and actuation.

This automatic protection is possible thanks to the natural behavior of the self-excited induction machine. As the current required by the load increases, especially in fault situations such as a short circuit, the terminal voltage progressively decreases [20]. This occurs because the abrupt increase in the load current causes a drop in the machine's magnetizing current, which is essential to maintain the magnetic flux required for voltage generation [51]. As a result, the system gives up and the output voltage collapses [20]. This behavior is highly desirable in clinical environments, as it significantly reduces the risks of electric arcs, conductor overheating, ignition of flammable materials, and damage to connected equipment. Moreover, the absence of voltage during the fault enhances the safety of patients and healthcare personnel, eliminating the need for complex protection systems.

This passive self-protection mode is verified in figure 4, where it can be observed that, as the load resistance value decreases, the current supplied increases up to the maximum power supplied, and after that the voltage tends to collapse. This behavior makes the system extremely safe and reliable.

5. Sizing methodology

This section presents the methodology for sizing a low-cost power generation system using a TIM to power a medical center in remote locations.

To ensure reliable system sizing, it is essential to determine the active and reactive power of the medical equipment set. These parameters directly influence the load on both the generator and the system's capacitors

Table 1 presents examples of medical equipment commonly found in medical stations, along with their typical active and reactive power values. Based on these values, the generator set used in this work is sized to accommodate maximum power demands of 320 W for active power, to be supplied by the TIM and prime mover, and 90 var for reactive power, which serves as the basis for sizing the capacitor bank.

5.1. Definition of induction generator

The safe selection of the TIM rated power to be used in the off-grid generation set is essential to ensure voltage stability, especially in critical applications such as medical equipment support systems. For this purpose, a sizing factor K_E is proposed, defined as the ratio between the maximum output power of the system $P_{\max} = 1800$ W—extracted directly from the critical point of the V_{out} versus P_{out} curve (figure 4)—and the rated power of the machine $P_{TIM} = 3000$ W:

$$K_E = \frac{P_{TIM}}{P_{\max}} = 1.66 \tag{17}$$

Thus, once the K_E factor has been determined for a specific topology, it becomes possible to apply it to the dimensioning of systems with other powers, as long as the same configuration conditions and machine class are respected. From this factor, the criterion is established that, in order to ensure safe operation and avoid demagnetization regimes, the TIM power to be used in the system must obey the following relationship:

$$P_{TIM} \geqslant P_{load} \cdot K_E \tag{18}$$

The definition of the factor K_E is therefore based on the identification of the point of the V_{out} versus P_{out} curve where the desired minimum voltage (in the assumption 220 V for sensitive equipment) is reached. This point is considered the maximum safe power that can be extracted from the machine for the adopted capacitance configuration (C_s 62.6% greater than C_p), being independent of the rated power of the machine. Thus, the definition of K_E is associated with the ratio between the rated power of the machine and its defined operational limit.

In addition, this approach is generalizable. Therefore, once the factor K_E for a specific topology is determined, it becomes possible to apply it to the dimensioning of systems with other power ratings, provided that the same connection conditions and machine class are maintained, as well as the same relationship between the magnetizing capacitances C_p and C_s. This occurs because the behavior of magnetization, voltage regulation and response to the load follow the same physical principle, characterized by the equations of the equivalent circuit presented in section 3 and by the electromagnetic characteristics of the machine.

On the other hand, for machines belonging to other classes (different magnetic saturation levels or efficiency), the numerical value of K_E changes. Nevertheless, the procedure to obtain the factor, based on the mathematical model and the analysis of the $V_{out} \times P_{out}$ curve, remains fully applicable. Thus, the proposed method enables the systematic determination of an appropriate sizing factor for different machines, avoiding empirical approaches commonly used in industrial practice.

5.2. Definition of prime mover

The prime mover, responsible for supplying the mechanical energy that will be converted into electrical energy by the TIM, must deliver mechanical power at the shaft exceeding the rated power of the generator, to ensure optimal performance of the engine (diesel os gasoline) and compensate for inherent system losses, including both mechanical and electrical losses associated with the generation process.

The minimum power required by the prime mover, P_{mec}, can be expressed as:

$$P_{mec} \geqslant \frac{P_{TIM}}{\eta_{TIM}} \cdot K_M \tag{19}$$

where η_{TIM} is the efficiency of the induction machine (typically between 85% and 92%), and K_M (value between 1.2 and 1.5) is the safety margin factor that must be applied to ensure that the prime mover does not operate close to its maximum load in steady state, which could compromise the reliability and useful life of the system.

5.3. Definition of capacitors

The capacitors must provide the reactive power required to magnetize the generator Q_{TIM}, and also the reactive power required for the loads connected to the system Q_{load} [52].

The empirical definition of the excitation capacitor bank can lead to several critical operational problems. For example, if the capacitance is undersized, the generator may not reach the self-excitation condition, resulting in insufficient and unstable terminal voltage. On the other hand, excessive capacitance can cause over-excitation, leading to high output voltage levels, magnetic saturation, increased harmonic distortion, and potential damage to both the generator and connected medical devices.

The connection topology used follows the method proposed by Fukami [26], which suggests connecting three capacitors in a star configuration to the machine terminals, as proposed in figure 1. Since the capacitors have different values, we can express the required reactive power provided by the unbalanced three-phase bank as:

$$3 \cdot Q_A = Q_{TIM} + Q_{load} \tag{20}$$

where Q_A is the average reactive power available for each phase of the three-phase system.

Assuming operation at 60 Hz, the losses associated with modern capacitors can be neglected. Thus, the voltage across each capacitor can be expressed as $V_{C_A} = X_{C_A} \cdot I_{C_A}$, where X_{C_A} is the capacitive reactance given by $X_{C_A} = \frac{1}{2\pi \cdot f \cdot C_A}$. With this simplification, it becomes possible to determine the required capacitance C_A so that the reactive power supplied to the system is satisfied, considering:

$$Q_A = V_{C_A} \cdot I_{C_A} = \frac{Q_{TIM} + Q_{load}}{3} = V_{C_A} \cdot \frac{V_{C_A}}{X_{C_A}} \tag{21}$$

By rearranging (21), it is possible to determine the minimum capacitance value, $C_{A\,\min}$, required for each phase of the capacitor bank, as follows:

$$C_{A\,\min} = \frac{Q_{TIM}}{3 \cdot 2\pi \cdot f \cdot V_{out}^2} \tag{22}$$

To determine the minimum capacitance value $C_{A\,\min}$ required to initiate self-excitation, it is first necessary to calculate the reactive power required by the TIM—using its specifications (table A1 in Appendix) –. Considering the power factor $\cos(\phi) = 0.77$, the phase shift angle $\phi \approx 39.65^\circ$ is obtained. With $P_{TIM} = 3.0$ kW, the reactive power is calculated as $Q_{TIM} = P_{TIM} \cdot \tan(\phi) = 2.486$ kvar. Considering the output voltage $V_{out} = 220$ V and assuming a system operating at frequency f, the minimum value of the excitation capacitance can be determined by (22), resulting in $C_{A\,\min} = 45.4\ \mu$F.

In this way, we can dimension the correct value of C_A according to the reactive power of the load Q_{load}, through (23), which provides flexibility for sizing the system:

$$C_A = C_{A\,\min} + \frac{Q_{load}}{3 \cdot 2\pi \cdot f \cdot V_{out}^2} \tag{23}$$

As detailed in [26], the capacitor values C_s are selected to minimize voltage regulation, with C_s being 62.6% greater than C_p. Therefore the values of C_p and C_s must satisfy the following condition:

$$\frac{2 \cdot C_s + C_p}{3} \geqslant C_A \tag{24}$$

With values close to C_A, the unbalanced three-phase bank is capable of supplying all the reactive power demanded by the system components, maintaining good voltage regulation and a wide operating power range, allowing resizing according to the needs of the equipment to be connected.

6. Experimental results

In figure 5, we observe the induction generator coupled to a induction motor, which acts as the prime mover of the system. In addition, the experimental setup includes a CFW500 frequency inverter, residual current switch, circuit breakers, 220-380 V autotransformer and associated capacitor bank, using $C_A = 53\ \mu$F according to the dimensioning proposed in section 5.3 following (23) and (24). The load profile includes the following equipment: 1 Alfamed brand multiparameter monitor, model Vita 400a; 1 Mindray brand cardioverter, model Beneheart 3D; 3 Terumo brand infusion pumps, model TE-LM 830.

Once the generator was excited and reached steady-state operation, the full load was applied, and potential interferences related to equipment operation were analyzed. The evaluation focused on voltage and current profiles, voltage regulation at the load, and the system's behavior under unbalanced operating conditions.

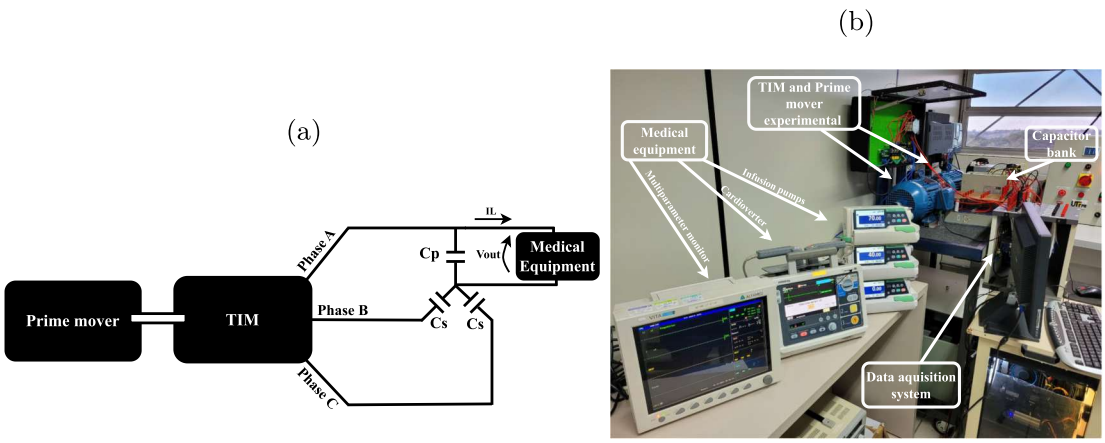

Figure 5. Proposed system: (a) simplified system diagram; (b) experimental setup.

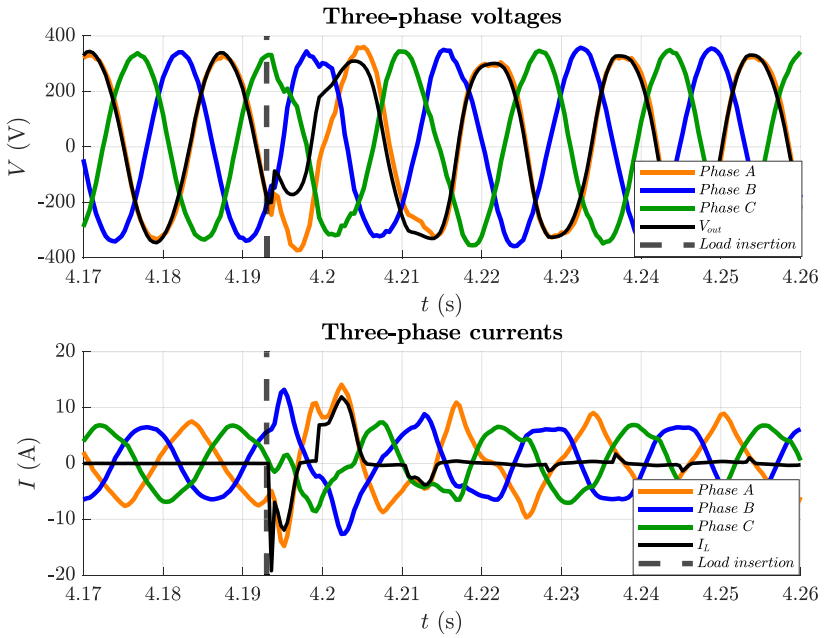

Figure 6. Insert load.

6.1. Transient analysis

Figure 6 shows the phase to neutral voltage and current waveforms in the generator windings when load is connected. The load insertion occurs near $t = 4.193$ s, marked by the vertical shaded area.

It can be seen that, before the load is applied, the three-phase voltages present a well-defined sinusoidal oscillation, with symmetrical amplitudes and a value of 242.7 Vrms, as depicted in figure 7, which validates the methodology described in the previous section. However, when the load is connected, a disturbance in the voltage waveform is observed. The voltage of one of the phases where the load is connected (phase A) undergoes damped oscillations before returning to a new steady state, with 224.2 Vrms, meeting the operational limits of medical equipment. This behavior demonstrates the transient response of the generator to a sudden load variation.

When the load is inserted, there is an increase in current in all phases, accompanied by transient oscillations. Three-phase currents maintain a sinusoidal profile similar to that of voltages, with moderate amplitude and which respects the operating limits of each winding of the machine. Figure 7 shows the value of the current supplied to the load with stability after the transient regime.

Figure 8 shows the variation in the system's output frequency under no-load operating conditions and after load connection. It can be observed that, before load application, the frequency remains stable at 60.12 Hz, demonstrating the stability of the prime mover drive.

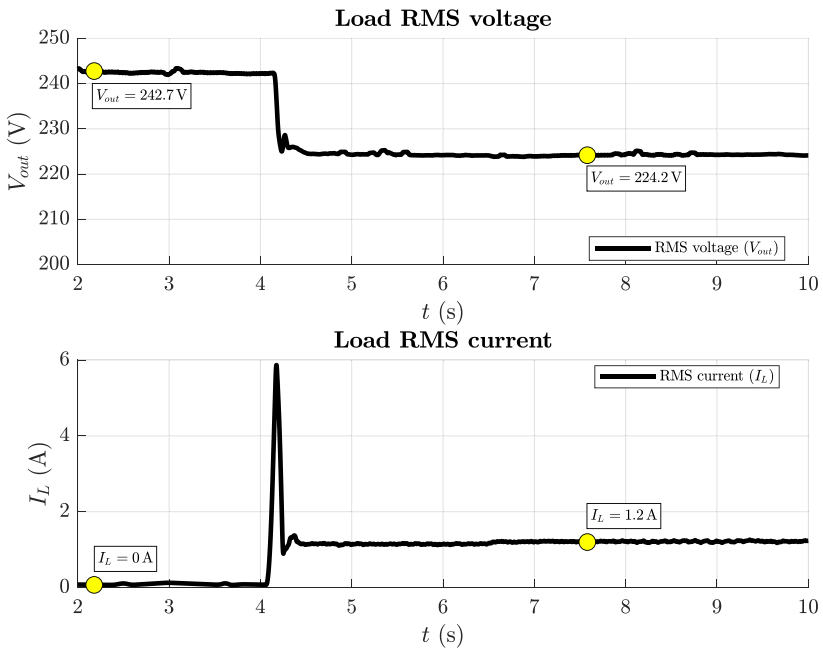

Figure 7. RMS voltage and current.

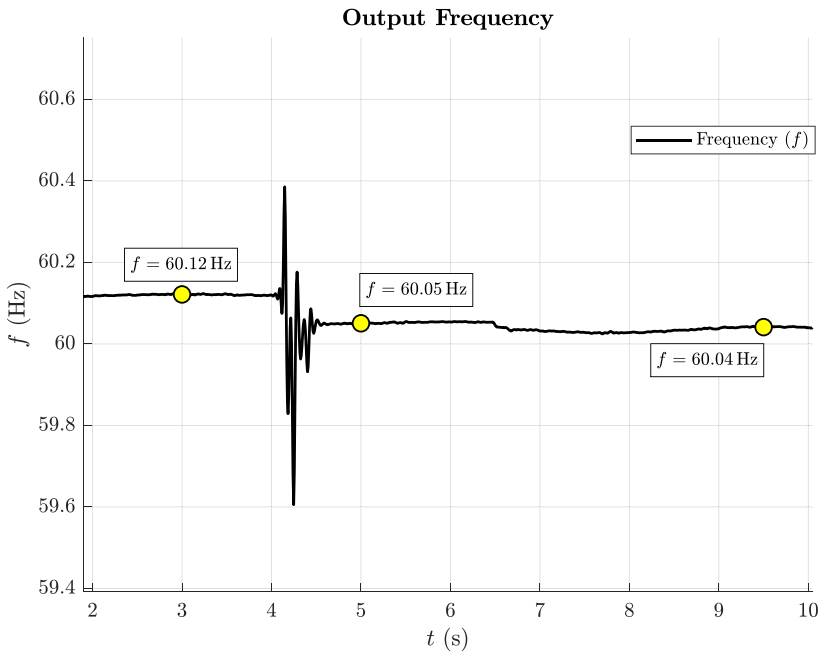

Figure 8. Output frequency.

At the instant of load connection, a short-duration transient occurs, characterized by small frequency oscillations associated with the electromechanical coupling between the SEIG and the applied load. This behavior is expected and is directly related to the distribution of mechanical and electrical power in the system, as well as the dynamics of the magnetizing current supplied by the capacitor bank.

After the transient, the frequency stabilizes rapidly, remaining close to 60 Hz, with values of 60.05 Hz under load and 60.04 Hz in prolonged steady state. This variation remains within acceptable limits for powering sensitive medical equipment, as discussed in section 2.

Although small transient frequency variations are observed during load events, the system demonstrates self-regulation capability, ensuring steady-state frequency stability, an essential aspect for clinical applications in isolated environments.

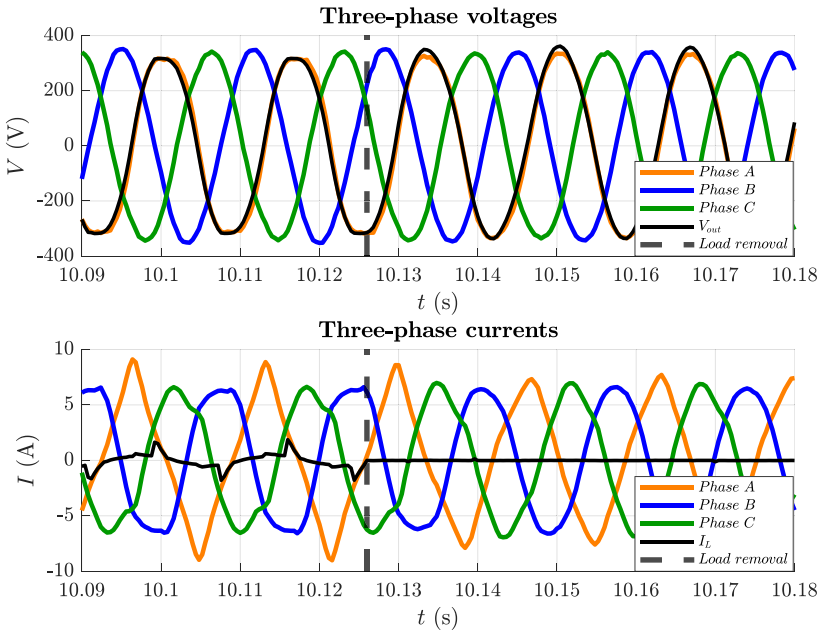

Figure 9. Load removed.

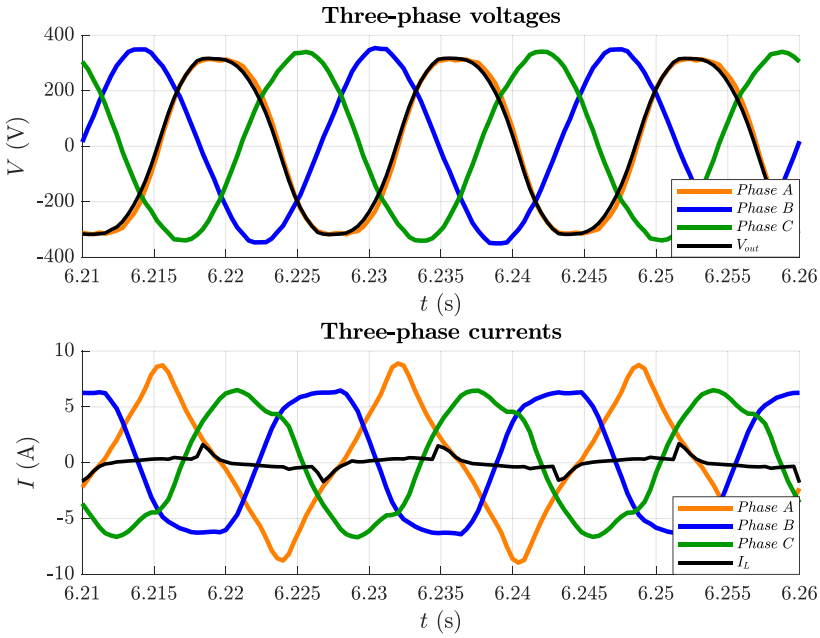

Figure 10. Steady-state operation of the TIM supplying a single-phase load.

Figure 9 represents the removal of the load from the system close to $t = 10.126$ s and shows that the voltages and currents gradually return to their no-load values, without abrupt oscillations or significant instabilities.

6.2. Steady-state analysis

After the load is applied, the generator reaches a new equilibrium state, characterized by a permanent and stable regime. Figure 10 illustrates the behavior of the output voltages in the three phases, showing small variations between them, but remaining within the recommended operational limits for the TIM used.

The harmonic analysis, through fast Fourier transform (FFT), of the output voltage of phase A to neutral is presented in figure 11.

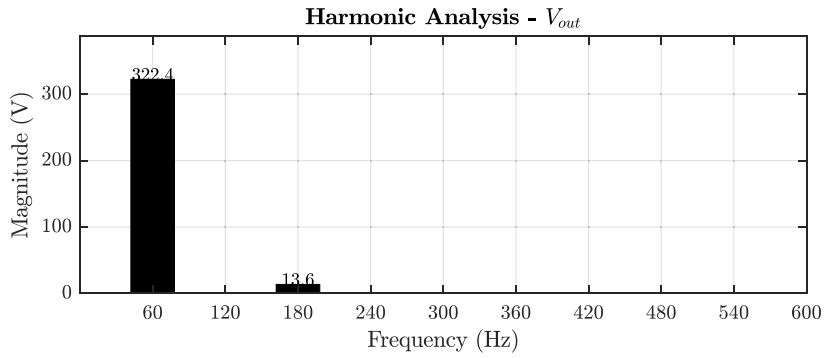

Figure 11. FFT of the phase A to neutral voltage.

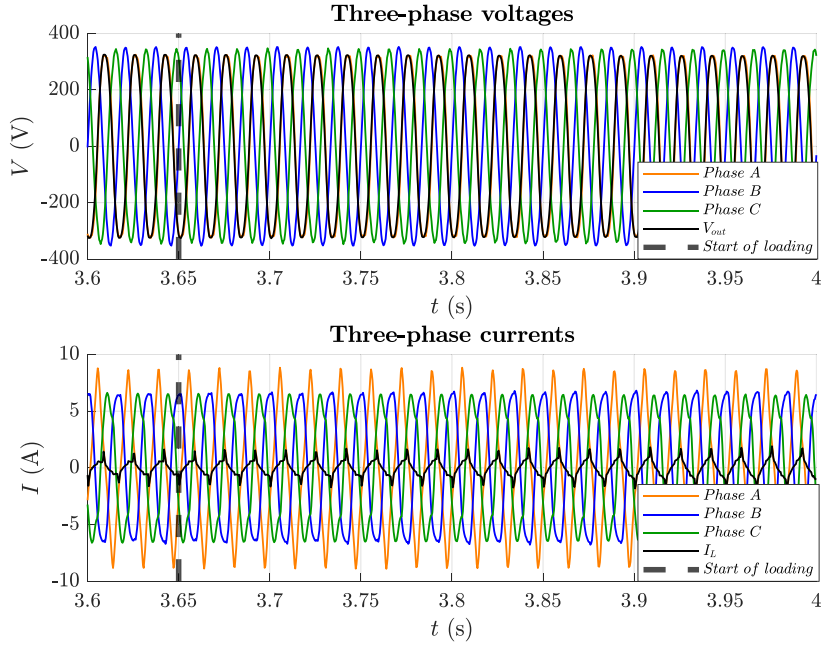

Figure 12. Beginning of cardioverter loading.

The total harmonic distortion (THD) for the voltage applied to the load can be calculated as: $THD_{v_{out}}(\%) = \frac{\sqrt{\sum_{n=2}^{\infty} V_n^2}}{V_1} \times 100 = 4.23\%$. The voltage was evaluated with medical equipment operating under normal operating conditions.

The value demonstrates that the distortion levels in the voltage applied to the load remained below the limits discussed in section 2, which reinforces the quality of the energy supplied. These results indicate that the interaction between the SEIG and the non-linear medical loads did not result in excessive waveform distortion. This result demonstrates that the excitation capacitance and inherent electromagnetic characteristics of the induction generator provide sufficient stiffness to limit harmonic propagation, even under active switching conditions of (Switched-Mode Power Supplies) SMPS-based equipment.

6.3. Cardioverter operation

Of all the devices tested, the cardioverter was the one with potential to affect the generator's performance; accordingly, a maximum discharge of 360 J was used to characterize its impact. The cardioverter's unique loading and unloading behavior was examined, as shown in figures 12 and 13, respectively.

At the beginning of loading (figure 12), there is a small gradual increase in load current, and an insignificant drop in generated voltage, which does not impact the operation of the system in steady state, and also does not present abrupt variations of transients.

The same is observed in figure 13, where we have the end of the loading process gradually and without significant variations. Thus, all voltages and currents return to their normal steady-state operation levels.

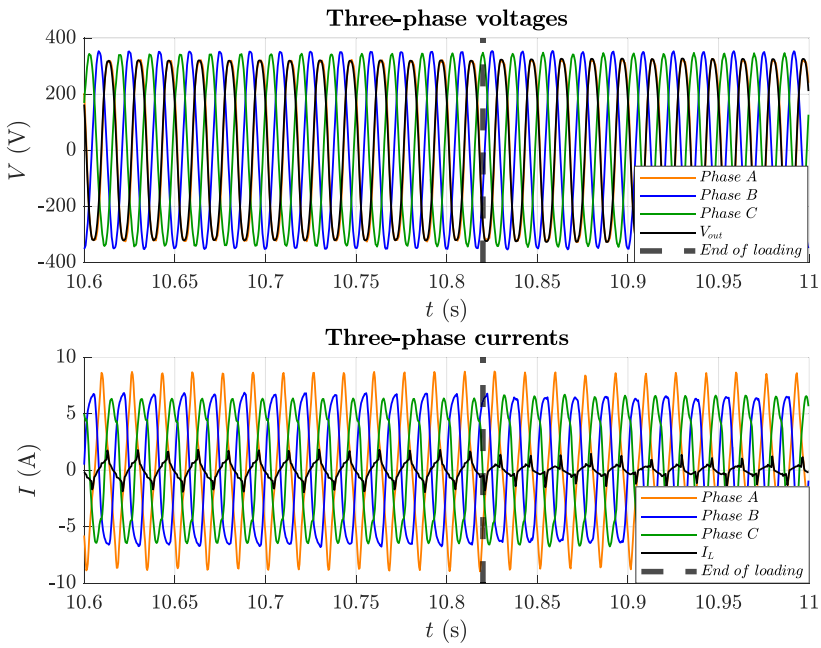

Figure 13. End of cardioverter loading.

After the charging process, the discharge was performed with the paddles in the equipment's tray for testing purposes. This operation did not demonstrate any impact on the voltage and current supply of the generator, which is attributed to the internal electronic circuits of the equipment itself. These stability characteristics are fundamental for the reliability of the system.

7. Conclusion

This work presented an innovative solution for providing reliable single-phase power to medical equipment in remote healthcare settings by utilizing a self-excited generator derived from a three-phase squirrel cage induction machine. Through comprehensive modeling, system design, and experimental validation, the study demonstrates that this approach ensures voltage stability, robust fault protection, and operational reliability without the need for complex or costly components. The component sizing methodology presented in section 5 proved effective in determining the excitation capacitance values that ensure reliable generator operation, avoiding under-excitation conditions, overvoltage phenomena, high levels of harmonic distortion, and other undesirable operating regimes. Furthermore, the proposed methodology is replicable and can be applied to systems with different power demands, allowing components to be properly sized according to the specific power requirements of the medical loads to be supplied, without relying on empirical adjustments.

The results indicate that the proposed system is practical, cost-effective, and capable of maintaining the proper functioning of critical medical devices under load transients, maintaining power quality requirements, making it a viable option for enhancing healthcare access in resource-constrained and off-grid environments.

Declarations

The data that support the findings of this study are available from the corresponding author upon reasonable request.

Human Ethics and Consent to Participate Declarations Not applicable

Competing Interests The authors declare no competing interests.

Clinical Trial Number Not applicable.

Consent for publication We, the authors, hereby grant permission for the publication of this manuscript in Engineering Research Express.

AI Disclosure AI models were used solely for experimental planning and not for drafting or reviewing parts of the manuscript.

Data availability statement

All data that support the findings of this study are included within the article (and any supplementary files).

Appendix. Features of induction machine

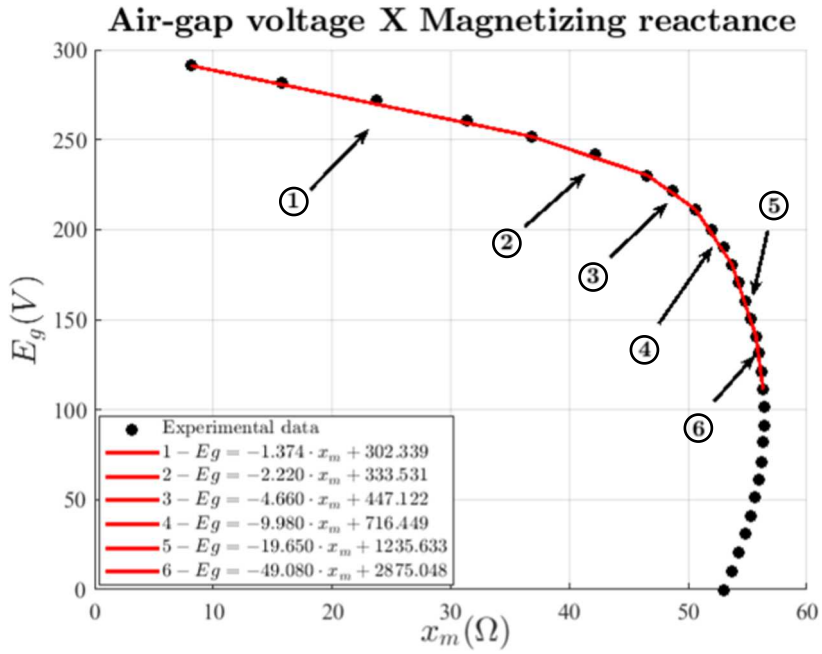

Figure A.1. Air-gap voltage as a function of the magnetizing reactance.

Table A1. TIM specifications.

Parameter	Value
Machine Type	3-phase squirrel-cage induction motor
Rated Power (P_{TIM})	4 HP $\approx$ 3 kW
Number of Poles	4
Power Factor ($\cos(\phi)$)	0.77
Service Factor	1.25
Efficiency (η_{TIM})	89.5%
Rated Frequency (f_r)	60 Hz
Rated Speed	1745 rpm
Voltage (Δ/Y)	220/380 V
Current (Δ/Y)	11.4/6.61 A
Stator resistance (r_1)	0.9911 Ω
Rotor resistance (r_2)	1.2697 Ω
Stator inductance (x_1)	6.04 Ω
Rotor inductance (x_2')	6.04 Ω

Author contributions

Bruno Romeiro 0009-0001-7694-0766
Data curation (equal), Formal analysis (equal), Investigation (equal), Methodology (equal), Software (equal), Validation (equal), Visualization (equal), Writing – original draft (lead), Writing – review & editing (equal)

Carlos Oliveira 0000-0001-8532-9769
Conceptualization (equal), Data curation (equal), Formal analysis (equal), Investigation (equal), Project administration (equal), Writing – review & editing (equal)

Cicero Hildenberg 0000-0002-0018-0561
Conceptualization (equal), Formal analysis (equal), Investigation (equal), Methodology (equal), Supervision (equal), Visualization (equal), Writing – original draft (equal), Writing – review & editing (equal)

Ângela Ferreira 0000-0002-1912-2556
Conceptualization (equal), Formal analysis (equal), Methodology (equal), Supervision (supporting), Visualization (equal), Writing – review & editing (equal)

Francisco Filho 0009-0003-7233-7315
Formal analysis (equal), Investigation (equal), Methodology (equal), Resources (equal), Software (equal), Visualization (equal)

References

[1] Ali M F, Islam Sheikh M R, Julhash M M and Sanvi A H 2025 Sustainable electrification of remote communities: techno-economic and demand response analysis for renewable microgrids *Energy Conversion and Management: X* **26** 100963
[2] Costa Canfild D, Siqueira J A C, Nogueira C E C, Santos R F, Tokura L K, Rossi A, Zanchet E and Orben J M C 2024 Comparative analysis between distributed generation and centralized electric power system to serve the inhabitants of remote areas of brazil *Observatório De La Economía Latinoamericana* **22** 3627
[3] Gama A S M, Fernandes T G, Parente R C P and Secoli S R 2018 Inquérito de saúde em comunidades ribeirinhas do amazonas, brasil *Cadernos de Saude Publica* **34** 2–3
[4] Castro L R C, Almeida F F S, Cavalcante A M S, Guimarães I R B, Silva V M, Lisboa F A M and Nascimento T V 2020 Panorama sanitário das populações ribeirinhas da amazônia brasileira e as tecnologias sociais aplicáveis *Research, Society and Development* **9** 5891210898
[5] Sharma L, Singh J, Dhiman R, Nunez D R V, Ba A E, Joshi K J, Modi B, Padhi A, Tandon J K and Seidel M 2024 Advancing solar energy for primary healthcare in developing nations: Addressing current challenges and enabling progress through unicef and collaborative partnerships *Cureus* **16** e51571
[6] Metello E, Silva F B, Monteiro R V A, Rondina J M and Guimarães G C 2024 Study of a self-excited three-phase induction generator operating as a single-phase induction generator for use in rotating excitation systems for synchronous generators *Energies* **17** 3900
[7] Cheng H, Huang W, Shen C, Peng Y, Shuai Z and Shen Z J 2021 Transient voltage stability of paralleled synchronous and virtual synchronous generators with induction motor loads *IEEE Trans. Smart Grid* **12** 4983–99
[8] Rao Y T, Chakraborty C and Basak S 2018 Brushless induction excited synchronous generator with induction machine operating in plugging mode *IEEE Trans. Ind. Appl.* **54** 5748–59
[9] Zhu H and Shen L 2023 Decoupling control of outer rotor coreless bearingless permanent magnet synchronous generator based on online least squares support vector machine inverse system and internal model controllers *Progress In Electromagnetics Research C* **128** 1–15
[10] Fukami T, Kaburaki Y, Kawahara S and Miyamoto T 1999 Performance analysis of a self-regulated self-excited single-phase induction generator using a three-phase machine *IEEE Trans. Energy Convers.* **14** 622–7
[11] Braga A V, Rezek A J J, Silva V F, Viana A N C, Bortoni E C, Sanchez W D C and Ribeiro P F 2015 Isolated induction generator in a rural brazilian area: field performance tests *Renew. Energy* **83** 1352–61
[12] Silva F B, Silva Gonçalves F A, Vanço W E, Carvalho D P, Bissochi C A, Monteiro R V A and Guimarães G C 2018 Application of bidirectional switches in the development of a voltage regulator for self-excited induction generators *International Journal of Electrical Power and Energy Systems* **98** 419–29
[13] Vanco W E, Silva F B, Oliveira C M R D, Monteiro J R B A and Oliveira J M M D 2019 A proposal of expansion and implementation in isolated generation systems using self-excited induction generator with synchronous generator *IEEE Access* **7** 117188–95
[14] Viorel A C and Crăciunaş G 2024 Single phase induction motor electrical performances *International Journal of Advanced Statistics and ITC for Economics and Life Sciences* **14** 169–75
[15] Chakraborty S and Pudur R 2022 A novel balancing operation topology for single-phase supply to remote locations from three-phase SEIG *IEEE 19th India Council International Conference (INDICON) (India)* (IEEE)
[16] Poddar G, Joseph A and Unnikrishnan A K 2003 Sensorless variable-speed controller for existing fixed-speed wind power generator with unity-power-factor operation *IEEE Trans. Ind. Electron.* **50** 1007–15
[17] Marra E G and Pomilio J A 1999 Induction generator based system providing regulated voltage with constant frequency *APEC '99. Fourteenth Annual Applied Power Electronics Conference and Exposition. 1999 Conference Proceedings (Cat. No.99CH36285)* 1 410–4151
[18] Murali Krishna V B, Sandeep V, Narendra B K and Prasad K R K V 2023 Experimental study on self-excited induction generator for small-scale isolated rural electricity applications *Results in Engineering* **18** 101182
[19] Chilipi R, Sumaiti A A and Singh B 2020 Control of self-excited induction generator-based micro-hydro power generation system feeding single-phase and three-phase loads *IEEE Industry Applications Society Annual Meeting* 1–8
[20] Reddy S 2021 Review of literature on self-excited induction generators and controllers *International Journal for Research in Applied Science and Engineering Technology* **9** 1576–87
[21] Ibtiouen R, Benhacine T Z, Mekhtoub S and Nesba A 2021 Low-cost three-phase self-excited induction generator for supplying isolated single-phase loads *International Journal of Digital Signals and Smart Systems* **5** 80
[22] Chan T F and Lai L L 2001 A novel single-phase self-regulated self-excited induction generator using a three-phase machine *IEEE Trans. Energy Convers.* **16** 204–8

[23] Ion C P and Marinescu C 2013 Three-phase induction generators for single-phase power generation: an overview *Renew. Sustain. Energy Rev.* **22** 73–80
[24] Chan T F and Lai L L 2002 Single-phase operation of a three-phase induction generator with the smith connection *IEEE Power Engineering Society Winter Meeting. Conference Proceedings (Cat. No.02CH37309)* **2** 1238–2
[25] Bansal R C 2005 Three-phase self-excited induction generators: an overview *IEEE Trans. Energy Convers.* **20** 292–9
[26] Fukami T, Imamura M, Kaburaki Y and Miyamoto T 1995 A new self-regulated self-excited single-phase induction generator using a squirrel cage three-phase induction machine *Proceedings 1995 International Conference on Energy Management and Power Delivery EMPD '95* 1 308–3121
[27] Gao S, Bhuvaneswari G, Murthy S S and Kalla U 2014 Efficient voltage regulation scheme for three-phase self-excited induction generator feeding single-phase load in remote locations *IET Renew. Power Gener.* **8** 100–8
[28] Chatterjee A and Chatterjee D 2016 Analysis and control of photovoltaic-assisted three-phase induction machine operating as single-phase micro-wind generator *IET Gener. Transm. Distrib.* **10** 2165–76
[29] Wang Y-J and Lee M-H 2012 A method for balancing a single-phase loaded three-phase induction generator *Energies* **5** 3534–49
[30] Nakorn P, Machot P, Kinnares V and Manop C 2021 Study of three-phase self-excited induction generator operating as single-phase induction generator supplying non-linear load *18th International Conference on Electrical Engineering/Electronics, Computer, Telecommunications and Information Technology (ECTI-CON)* 806–9 10.1109/ECTI-CON51831.2021.9454845
[31] Yukhalang S, Sopapirm T and Kinnares V 2023 Three-phase self-excited induction generator operating as single-phase induction generator using static var compensator *20th International Conference on Electrical Engineering/Electronics, Computer, Telecommunications and Information Technology (ECTI-CON)* 1–7
[32] Syukri M, Syuhada A, Akhyar A and Tarmizi T 2025 Performance improvement of self-excited induction generator using capacitor bank based on pid controller *Radioelectronic and Computer Systems* **2025** 199–210
[33] Zine-Eddine B T, Ali N, Said M and Rachid I 2018 A balancing method for three-phase seig feeding a single-phase load by using switched capacitors *International Conference on Electrical Sciences and Technologies in Maghreb (CISTEM)* 1–6
[34] Kumar V 2022 Aspects of three phase induction generator in single-phase operation in terms of power quality *2nd International Conference on Power Electronics & IoT Applications in Renewable Energy and Its Control (PARC)* 1–4
[35] Mahato S N, Singh S P and Sharma M P 2008 Excitation capacitance required for self excited single phase induction generator using three phase machine *Energy Convers. Manage.* **49** 1126–33
[36] Chakraborty S, Samanta J and Pudur R 2024 Experimental analysis of a modified scheme for supplying single-phase remote loads from micro-hydro based three-phase self-excited induction generator *Measurement: Sensors* **33** 101166
[37] Westphal G A, Fernandes V, Westphal V, Fonseca J C, Silva L R and Valiatti J L D S 2020 Use of cpap as an alternative to the apnea test during the determination of brain death in hypoxemic patients. report of two cases *Revista Brasileira de terapia intensiva* **32** 319–25
[38] World Health Organization 2023 *Energizing Health: Accelerating Electricity Access in Health-care Facilities* (World Health Organization)
[39] Atanda O, West J, Stables T, Johnson C, Merrifield R and Kinross J 2023 Flow rate accuracy of infusion devices within healthcare settings: a systematic review *Therapeutic Advances in Drug Safety* **14** 20420986231188602
[40] Rasouli M and Phee S 2010 Energy sources and their development for application in medical devices *Expert Review of Medical Devices* **7** 693–709
[41] Ibáñez-Cruz A, Espinoza-Morriberon D, Vergara-Florián A and Algoner W 2025 Analysis and mitigation of fire and explosion hazards in hospital environments from a biomedical engineering perspective *Frontiers in Built Environment* **10** 1495594
[42] Fares B, Abdelli R and Bouzida A 2024 Performance analysis of a self-excited induction generator under unbalanced load *2nd International Conference on Electrical Engineering and Automatic Control (ICEEAC)* 1–6
[43] Santoso H, Wibawa U, Subroto R K and Ardhenta L 2018 Impact of load and speed variation to frequency variation on single-phase self-excited induction generator *Electrical Power, Electronics, Communications, Controls and Informatics Seminar (EECCIS)* 5–8
[44] Chan T F 1995 Analysis of self-excited induction generators using an iterative method *IEEE Trans. Energy Convers.* **10** 502–7
[45] Chandran V P and Vadhera S 2011 Capacitance requirements of self excited induction generator for different operating conditions *International Conference on Energy, Automation and Signal* 1–6
[46] Al-Senaidi S H, Alolah A I and Alkanhal M A 2018 Magnetization-dependent core-loss model in a three-phase self-excited induction generator *Energies* **11** 3228
[47] Nasir B A 2022 Dynamic modeling of wound-rotor slip-ring induction generator with switched-excitation capacitance and chopper resistance across bridge rectifier in the rotor circuit *European Journal of Electrical Engineering* **24** 27–32
[48] Tiwari H P and Diwedi J K 2002 Minimum capacitance requirement for self-excited induction generator *National Power Systems Conference (NPSC 2002)* (Indian Institute of Technology) *(Kharagpur, India)* 5–10
[49] Ofualagba G and Ubeku E U 2011 The analysis and modelling of a self-excited induction generator driven by a variable speed wind turbine ed R Carriveau *Fundamental and Advanced Topics in Wind Power* (IntechOpen) Chap. 1110.5772/18159
[50] Tawfiq K, Abdou A F, EL-Kholy E E and Shokralla S S 2017 A modified open loop control of a matrix converter connected to wind energy system *Renewable Energy and Sustainable Development* **3** 175–82
[51] Makowski K and Leicht A 2018 Behaviour of single-phase self-excited induction generator during short-circuit at terminals *COMPEL-The International Journal for Computation and Mathematics in Electrical and Electronic Engineering* **37** 1815–23
[52] Simone G A 2009 *Máquinas de Indução Trifásicas - Teoria e Exercícios* 2nd edn (Érica, São Paulo) E-book 216–7 Disponível em (https://app.minhabiblioteca.com.br/reader/books/9788536519814/)